RESEARCH ARTICLE

Gamma-band auditory steady-state response after frontal tDCS: A double-blind, randomized, crossover study

Yoshiaki Miyagishi[1], Takashi Ikeda[2]*, Tetsuya Takahashi[3], Kiwamu Kudo[4], Hirofumi Morise[4], Yoshio Minabe[1,2], Mitsuru Kikuchi[2]

1 Department of Psychiatry and Neurobiology, Graduate School of Medical Science, Kanazawa University, Kanazawa, Japan, **2** Research Center for Child Mental Development, Kanazawa University, Kanazawa, Japan, **3** Health Administration Center, University of Fukui, Fukui, Japan, **4** Ricoh Institute of Future Technology, Research and Development Division, Ricoh Company, Ltd., Kanazawa, Japan

* tikeda@med.kanazawa-u.ac.jp

Abstract

The effects of transcranial direct current stimulation (tDCS) likely depend on cortical N-methyl-D-aspartic acid (NMDA) neurotransmission; however, no previous studies have reported tDCS-mediated modulation of cortical NMDA neurotransmission in humans. The gamma-band auditory steady-state response (ASSR) to a 40 Hz stimulation likely reflects the integrity of cortical NMDA neurotransmission. The present study tested whether the effect of tDCS is reflected in gamma-band ASSRs during a 40 Hz stimulation. Using a double-blind, randomized, crossover study, we performed magnetoencephalography (MEG) and measured the ASSR in 24 healthy participants during 40 Hz of auditory stimulation after prefrontal tDCS (2 mA) or sham (i.e., placebo) treatment. Our results failed to reveal significant differences in any brain between the two conditions after the application of a frequency of approximately 40 Hz. Based on these results, the ASSR is an insufficient method to detect the effect of tDCS on cortical NMDA neurotransmission. Unexpectedly, the results revealed an enhanced beta-band event-related spectral perturbation (ERSP) in the left motor cortex after tDCS compared with that observed after the sham stimuli. Given that beta-band oscillations reflect many functions in motor cortices, the tDCS for the frontal areas had some effect on the left motor cortex while the participants were focusing on not pressing the button with their right index finger. An additional study with an adequate psychological task is necessary to draw a conclusion regarding this unexpected result.

Introduction

Transcranial direct current stimulation (tDCS) is a form of electrical neuro-stimulation [1]. To date, tDCS has been used to treat a variety of psychiatric (e.g., major depressive disorder and schizophrenia) and neurological conditions [2–5], and it has been used to alter performance on a range of cognitive tasks [6, 7]. According to the results of an animal study, anodal

stimulation applied directly to the cortex increases the positive character of the resting membrane potential, whereas cathodal stimulation causes hyperpolarization [8]. Previous neuroimaging studies of humans revealed that anodal stimulation tends to increase the blood oxygen level-dependent (BOLD) signal, whereas cathodal stimulation decreases this signal [9, 10]. Intriguingly, many previous studies have reported the effectiveness of left dorsolateral prefrontal anodal tDCS as a treatment for major depressive disorder [4, 5] and schizophrenia [11], as well as working memory performance in healthy subjects [7].

tDCS is associated with the modulation of glutamatergic, gamma-aminobutyric acidergic (GABAergic), dopaminergic, serotonergic, and cholinergic activities [12]. These modulations likely affect plasticity processes, making tDCS an important tool for clinical treatment and for understanding cognitive ability. Notably, previous pharmacological studies using transcranial magnetic stimulation revealed that the effects of tDCS depend on cortical N-methyl-D-aspartic acid (NMDA) neurotransmission and the $GABA_A$ receptor [13, 14]; however, no previous studies have investigated whether tDCS of the frontal area modulates cortical NMDA neurotransmission in humans.

The auditory steady-state response (ASSR) is an electro-magneto-physiological response entrained to both the frequency and phase of rapid and periodic auditory stimuli [15] and is typically captured using noninvasive techniques such as electroencephalography (EEG) and magnetoencephalography (MEG). This response is most evident in humans when stimuli are presented in the gamma frequency range (30–50 Hz) [15]. Notably, the ASSR in the gamma frequency range is likely the most robust finding of abnormal gamma oscillations recorded by either EEG [16–23] or MEG [24–28] in patients with schizophrenia [29]. In addition, the ASSR recorded by EEG during 40 Hz of stimulation likely reflects the integrity of cortical NMDA neurotransmission [30, 31].

MEG has been in development for human use since the 1960s, and its development has been greatly aided by EEG studies and recent advances in computational algorithms and hardware [32]. EEG-sensing technology is extremely mature (over 80 years of history) and relatively cost effective compared with other neuroimaging devices. MEG has a relatively short history and is generally very expensive. However, evidence from healthy populations (comparing the sensitivity of EEG to MEG for the measurement of gamma-band oscillations) has highlighted the improved detectability of high-frequency activity (i.e., gamma-band oscillation) using MEG measurements [33]. Recent evidence suggests that an MEG-informed reconstruction of the source significantly enhances the signal-to-noise ratio of 40-Hz ASSR estimates during normal brain functioning [34]. To our knowledge, however, no previous MEG studies have investigated the effect of tDCS on gamma-band ASSRs in humans. The present study tested whether gamma-band ASSRs are altered after tDCS (left frontal anodal tDCS).

Materials and methods

Participants

Twenty-four right-handed adult male students (mean age = 21.3, range = 20–23 years old) were recruited from Kanazawa University and participated in this experiment. All participants were native Japanese speakers with normal hearing and had no medical or family histories of neurological or psychiatric disorders. The full IQ score was estimated using the Japanese version of the National Adult Reading Test (mean = 108.4, range 93–120) [35]. These men agreed to participate in this study with full knowledge of the experimental nature of the research. Each participant provided written informed consent prior to participation. The Ethics Committee of Kanazawa University approved this study, which conformed to the tenets of the Declaration of Helsinki.

Experimental design

The study employed a randomized double-blind controlled placebo (active tDCS, sham) cross-over design that included an interval of at least one month (mean interval = 57.4 days). At the beginning of the experiment, participants were randomly assigned to either the active tDCS or sham stimulation condition. Ten minutes (the preparation time for MEG measurement) after stimulation, we measured the neuromagnetic ASSR to investigate the effect of tDCS (Fig 1).
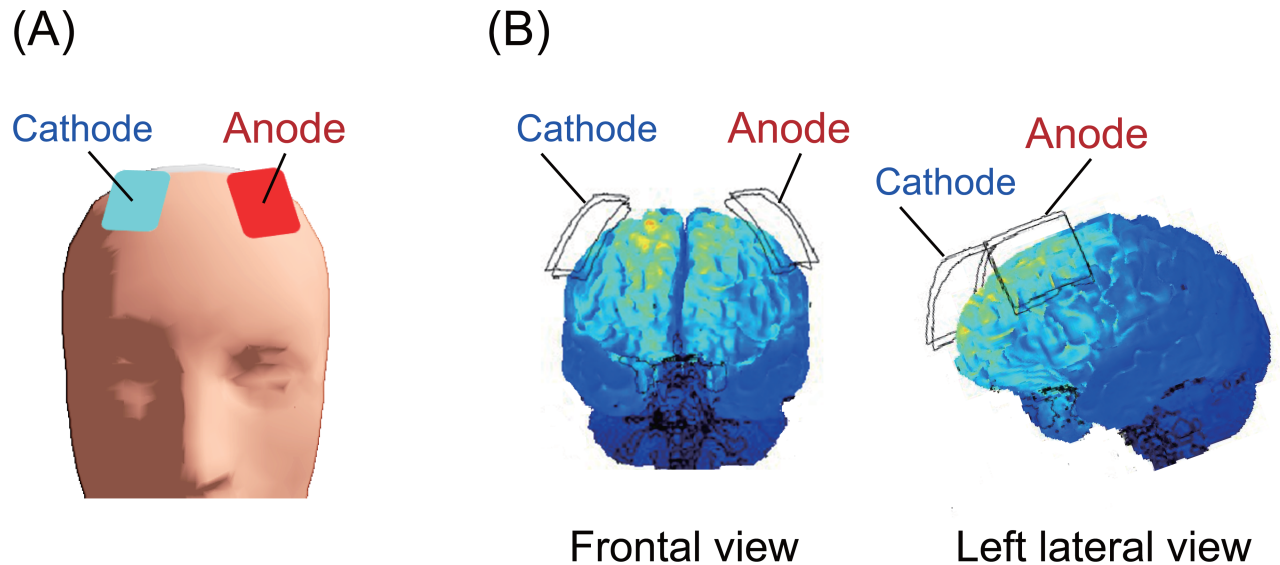
tDCS

A direct current was induced through two saline-soaked surface sponge electrodes (35 cm^2) and delivered using a battery-driven, constant current stimulator (DC-STIMULATOR Plus, neuroConn GmbH, Germany). The anode electrode was placed over F3, and the cathode electrode was placed over F4 (see the international EEG 10/10 system) during stimulation (Fig 2). Participants received the stimulus twice, and the duration of the stimulation was 13 minutes at a current strength of 2 mA to maximize the subsequent effects of stimulation. Twenty minute inter-stimulation intervals were employed between stimuli [36]. During the sham stimulation, electrodes were also attached to the participant, but the current was only delivered during the first 10 seconds, which prevented the participants from noticing the absence of electrical stimulation.
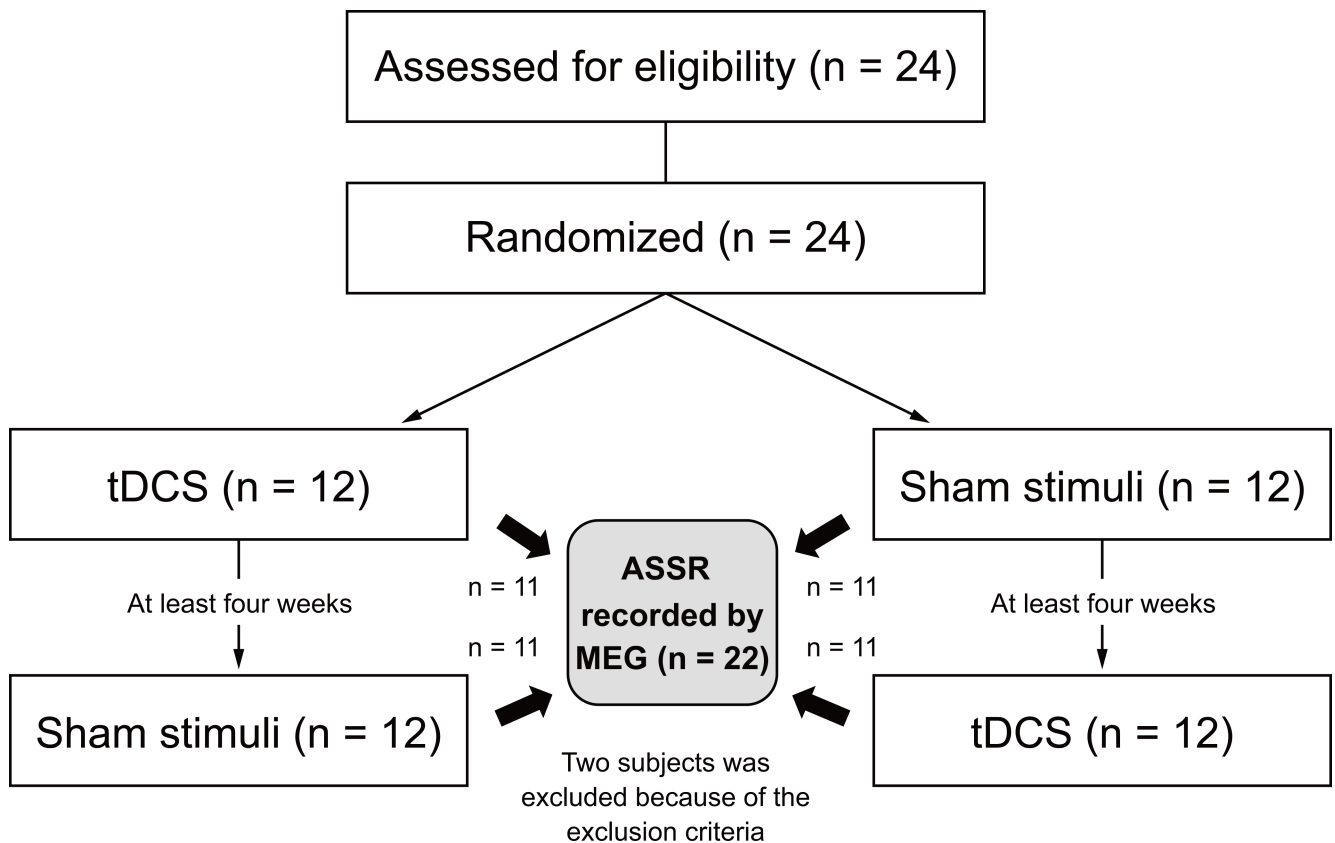
Fig 1. Study design: A double-blind, randomized, crossover study. Twenty-four participants were recruited and randomly assigned to receive either tDCS or sham stimulation during the first trial. After an interval of at least four weeks, the second trial was conducted. The order of the two stimulation conditions (i.e., tDCS or sham) was counterbalanced across participants. After delivering one of the two stimulus conditions, ASSRs were recorded using MEG. We excluded two participants from the statistical analysis because they met the exclusion criteria. ASSR, auditory steady-state response.

Fig 2. Electrode placement. (A) Anodal (F3) and cathodal (F4) electrodes marked on the scalp surface. (B) The computational simulation of brain current flow during the delivery of the tDCS. Major changes in the brain current flow were observed in the dorsal-frontal areas during stimulation [37].

ASSR

The ASSR session included passive listening tasks in which 250 trials of click-train stimuli were presented binaurally at 80 dB sound pressure level for 1000 ms each, with an inter-trial interval of 2000 ms. The click-train stimulus was a series of 1 kHz single sine-wave stimuli administered at a stimulation frequency of 40 Hz. The stimuli were received using stereo earphones with earplugs (ER-30, Etymotic research Inc., IL, USA). During the scan, participants were instructed to look at a white fixation cross on a black background presented on the screen in front of them. Participants were required to perform one task to confirm their awake state. Their task was to detect the 2 kHz click-train stimulus presented ten times during the session (the button press cue proportion was 4%). When the 2 kHz stimulus was presented, participants pressed a button (LUMINA LU400-PAIR, Cedrus Corporation, CA, USA) with their right index fingers. All stimuli were controlled using Presentation (Version 13.1, Neurobehavioral Systems, CA, USA) for Windows XP. A trigger signal was sent to an MEG recording system to indicate the start of the sound stimulus.

Data acquisition

Magnetic fields were measured using a whole-head-type system for adults at a laboratory within Ricoh Company in Japan. This system (MEGvision PQA160C; Ricoh Company, Ltd., Kanazawa, Japan) consisted of 160 channels. Sensors were configured as first-order coaxial gradiometers with a baseline of 50 mm; each coil of the gradiometers measured 15.5 mm in diameter. Magnetic fields were sampled at 2000 Hz per channel with a 500 Hz low-pass filter. Using a Signa Excite HD 1.5 T system (GE Yokogawa Medical Systems Ltd., Milwaukee, WI, USA), we obtained a T1-weighted structural image with spherical lipid markers placed at the 5 MEG fiduciary points to enable us to superpose the MEG coordinate system on the MRI data. A T1-weighted image consisted of 166 sequential 1.2 mm-thick slices with a resolution of 512×512 points within a field of view of 261×261 mm. The cortex surface was reconstructed using Freesurfer (version 5.3, http://surfer.nmr.mgh.harvard.edu/).

MEG data analyses and statistics

All data processing and analytical procedures were performed using Brainstorm [38], and additional scripts were developed using MATLAB® (The MathWorks, Natick, MA, USA). Noisy or flat channels were eliminated from the analysis. Eye-movement and cardiac artifacts were removed using the signal-space projection (SSP) method. Segments that included head movement or muscle artifacts detected in a visual inspection or the automatic processing procedure in Brainstorm were discarded. The epoch was defined as -500 to 1500 ms relative to the auditory stimulus onset (0 ms). Data were then baseline-corrected with respect to the mean of the prestimulus period (from -500 to 0 ms).

We estimated the signal source using the anatomy of each subject. The lead field was then computed using the overlapping spheres algorithm [39], with a cortical surface tessellated with 15,000 vertices. The inverse solution was calculated for each individual using sLORETA [40]. A noise covariance matrix was calculated based on the MEG recordings obtained during the -500 to 0 ms time window of every epoch within a session. Regions of interest (ROIs) were determined based on the Desikan-Killiany gyrus atlas segmented by Freesurfer.

A time-frequency analysis was conducted using Morlet wavelets with a central frequency of 2 Hz; a time resolution of 3 s was chosen for the mother wavelet. We calculated the event-related spectral perturbation (ERSP) and inter-trial phase coherence (ITPC) from 2 to 50 Hz. The ERSP represents the event-related percent changes in signal magnitude relative to a prestimulus baseline period (from -200 to 0 ms). The ITPC was calculated using complex values based on the raw output from the time-frequency analysis function of Brainstorm, and it indicates the phase consistency across trials. The time-frequency maps of all ROIs are shown in supporting information S1 Fig (ERSP) and S2 Fig (ITPC).

Statistics

To compare the neural activation under the tDCS and sham conditions, we conducted paired *t*-tests (21 degrees of freedom) for each ROI within each time frame from 0 to 1500 ms and for each frequency frame from 2 to 50 Hz. The threshold for statistical significance was set to $p < 0.05$, with a false discovery rate (FDR) correction across all 68 ROIs and 49 frequency dimensions. The same procedure was applied to the analyses of ERSP and ITPC data.

Results

Two of the 24 participants were excluded. One participant was excluded from further analysis because of drowsiness during the MEG recording. The other participant was excluded because of magnetic contamination from a tooth filling. Ultimately, twenty-two participants completed all sessions (Fig 1). The mean estimated IQ score in the twenty-two participants was 107.7 (range 93–120).

ERSP in the 40 Hz ASSR

An ERSP at approximately 40 Hz was clearly observed in most ROIs during 40 Hz of auditory stimulation under both the tDCS and sham conditions. A representative ERSP at approximately 40 Hz is shown in the transverse temporal gyrus in Fig 3. Paired-sample t-tests failed to identify significant differences in ERSPs at approximately 40 Hz in any of the ROIs when the statistical threshold was set to $p < 0.05$ with FDR corrections across ROIs and frequency dimensions (Fig 4; upper row).

ERSP in transverse temporal gyrus
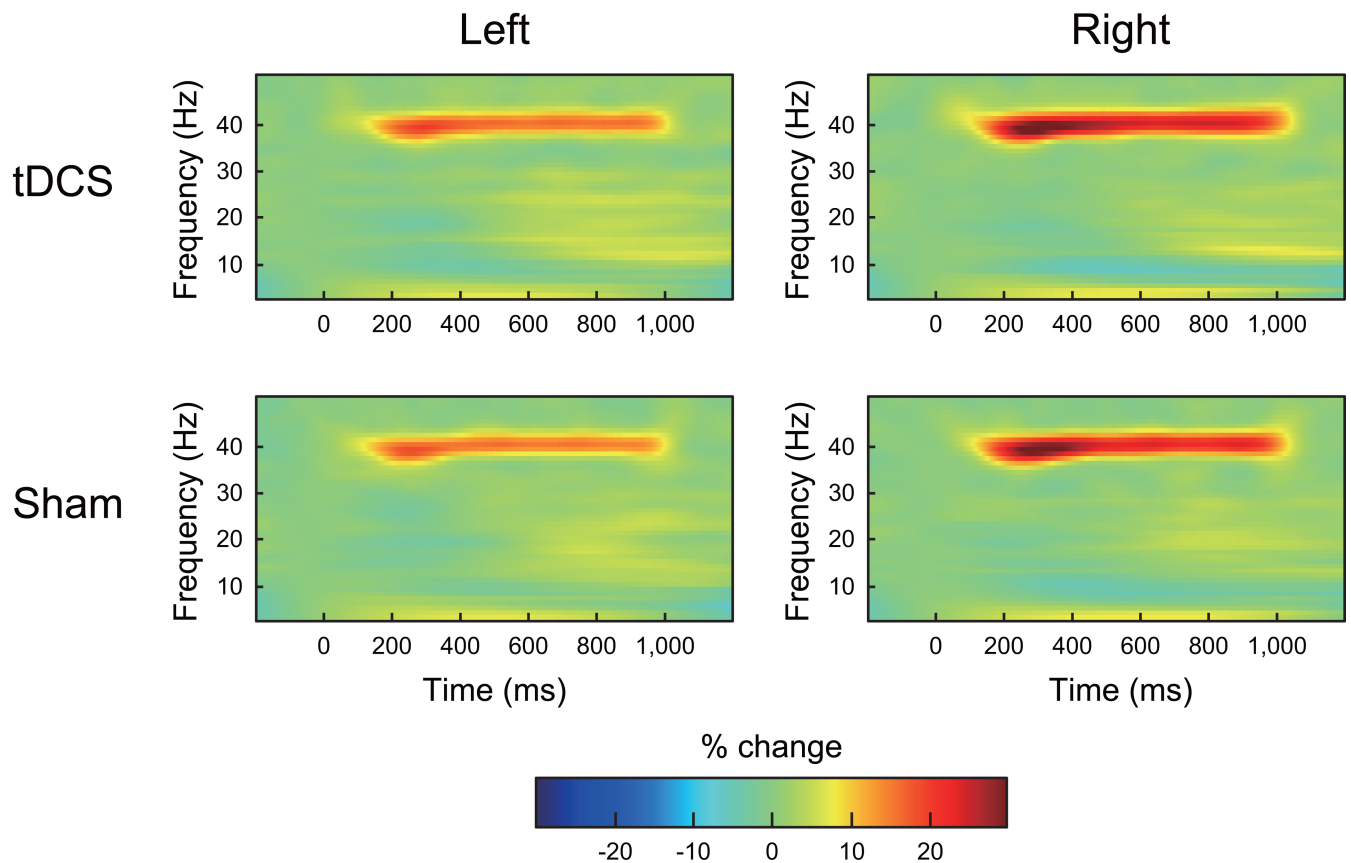
Fig 3. The grand average of the time-frequency maps of the ERSP in the transverse temporal gyrus under both tDCS and sham conditions. In each map, the x-axis indicates time (ms), and the y-axis indicates frequency (Hz). The color indicates the ERSP at each time-frequency point (reflected as the percentage change from baseline). The gamma-band (40 Hz) ASSR derived from the 40 Hz auditory stimulation was clearly observed under the tDCS and sham conditions.

https://doi.org/10.1371/journal.pone.0193422.g003

ITPC in the 40 Hz ASSR

An ITPC at approximately 40 Hz was clearly observed in most of the ROIs during the 40 Hz auditory stimulation under both the tDCS and sham conditions. A representative ERSP at approximately 40 Hz is shown in the transverse temporal gyrus in Fig 5. Paired-sample t-tests failed to identify significant differences in ERSPs at approximately 40 Hz in any of the ROIs when the statistical threshold was set to $p < 0.05$ with FDR corrections across ROIs and frequency dimensions (Fig 4; lower row).

ERSPs and ITPCs in other bands

Outside of the gamma-band range, paired-samples t-tests unexpectedly revealed an enhanced beta-band ERSP in the left motor cortex (precentral gyrus) after tDCS compared with that observed after the sham stimuli (Fig 6A; highlighted with a red rectangle). Fig 6B shows the ERSP in the left precentral gyrus. No significant differences in ITPCs were observed in any bands for any ROIs.

ERSP *t*-mapping (tDCS vs Sham)
in transverse temporal gyrus
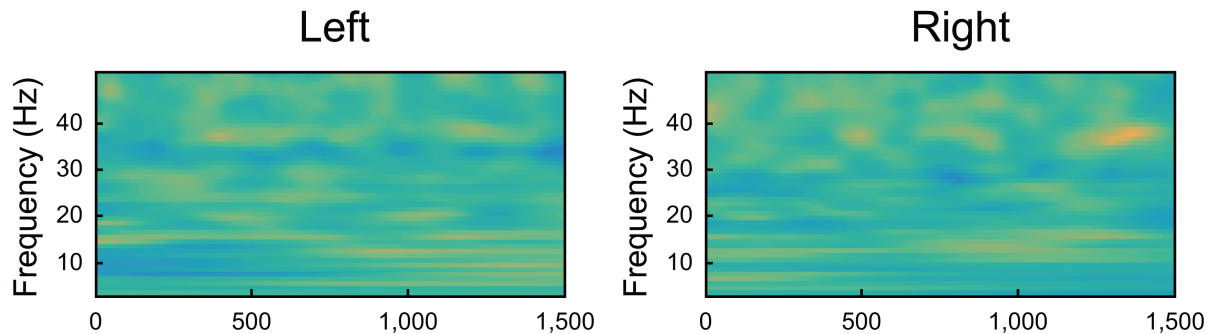
# ITPC *t*-mapping (tDCS vs Sham)
in transverse temporal gyrus
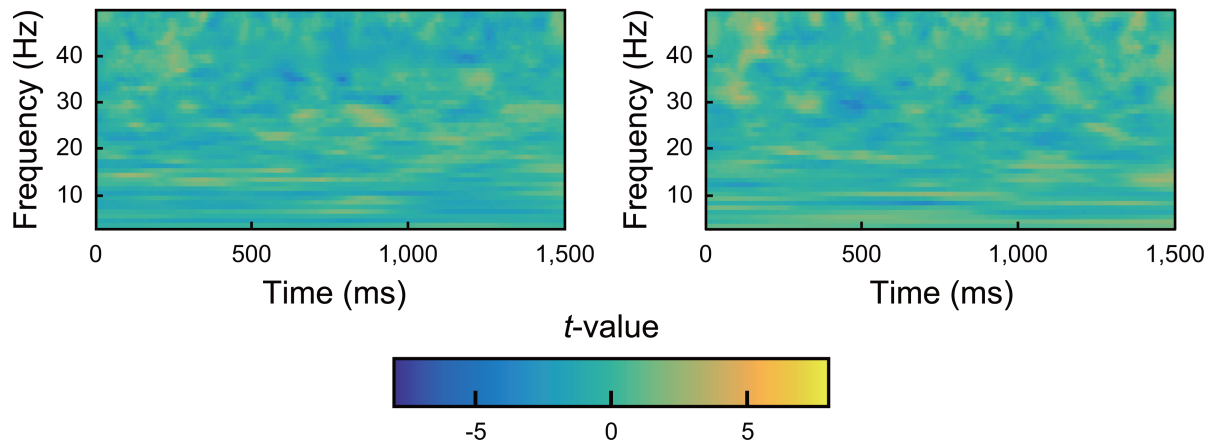
Fig 4. *T*-maps of the differences in ERSPs (upper row) and ITPCs (lower row) in the transverse temporal gyrus between the tDCS and sham conditions. Color indicates *t*-values at each time-frequency point. No significant differences were found in either ERSPs or ITPCs when the statistical threshold was set to $p < 0.05$ with an FDR correction.

Discussion

To our knowledge, this study is the first to investigate the effects of frontal tDCS on gamma-band ASSRs in humans. However, we failed to observe a significant effect of tDCS (left frontal anodal tDCS) on either ERSPs or ITPCs in the gamma-band for any ROI. Based on these results, a 40 Hz ASSR is insufficient to detect the effect of tDCS on cortical NMDA neurotransmission. One possible explanation might include the lack of statistical power needed to detect the subtle effect of tDCS on cortical NMDA neurotransmission. In addition, the gamma-band ASSR used in the present study might have been inadequate to detect subtle changes in NMDA neurotransmission induced by tDCS. Alternatively, tDCS might not have a specific effect on cortical NMDA neurotransmission, although this hypothesis is inconsistent with the results of previous pharmacological studies [13].

Unexpectedly and intriguingly, we observed an enhanced beta-band ERSP in the left motor cortex after tDCS compared with that observed after the sham stimuli. This enhanced
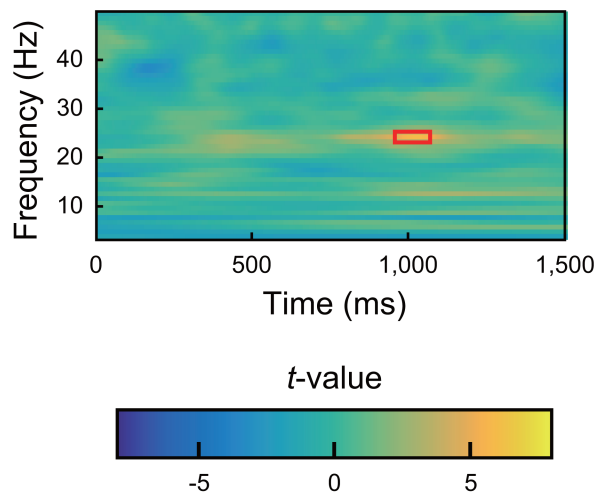
ITPC in transverse temporal gyrus
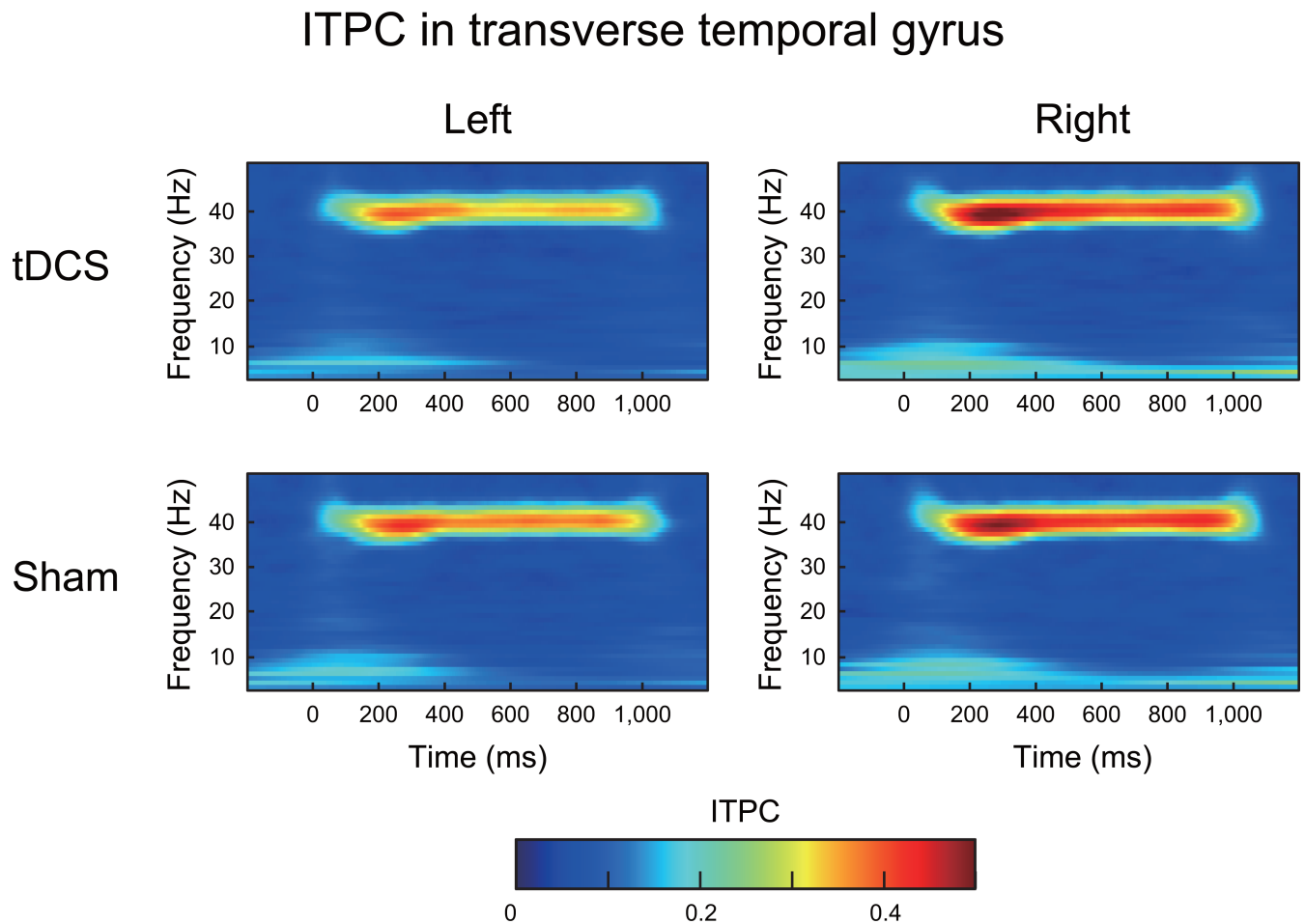
Fig 5. The grand average of the time-frequency maps for the ITPC in the transverse temporal gyrus under both tDCS and sham conditions. In each map, the x-axis indicates time (ms), and the y-axis indicates frequency (Hz). The color indicates the ITPCs at each time-frequency point. The ITPC peak in the gamma-band (40 Hz) was clearly observed during the 40 Hz auditory stimulation.

https://doi.org/10.1371/journal.pone.0193422.g005

beta-band ERSP in the left motor cortex (precentral gyrus) might reflect the inhibition of cortical activity by tDCS. Go/No-Go paradigms consist of a series of stimulus-induced movements in which the subject must decide whether to move depending on the characteristics of the stimulus. These paradigms have been extensively used to study processes linked to decision making and response inhibition. Usually, the behavioral index of inhibitory control is the number of errors a subject makes on the No-Go trials (i.e., false alarms [FAs]). In the present study, participants were required to detect the deviant click-train stimulus presented ten times in a session. When the deviant stimulus was presented, participants were required to press a button with their right index fingers (the proportion of Go tasks was 4%), and they were required to fail to respond to the standard stimulus (the proportion of No-Go tasks was 96%). Therefore, we might regard our ASSR session as an atypical Go/No-Go task, and the enhanced beta-band ERSP in the left motor cortex might reflect the No-Go task-related cortical activity modulated by tDCS. However, the behavioral results did not reveal an effect of tDCS on the Go/No-Go performance. In the present study, the FA means (range) per stimulation were 0.20 (0–0.8) and 0.38 (0–1.6) for the tDCS and sham conditions, respectively, and no significant differences in the number of FAs were observed between the two conditions (Wilcoxon signed-rank test, $z = 1.34$, $p > 0.05$).

(A) ERSP *t*-mapping
(tDCS vs Sham)
in left precentral gyrus

(B) ERSP in left precentral gyrus
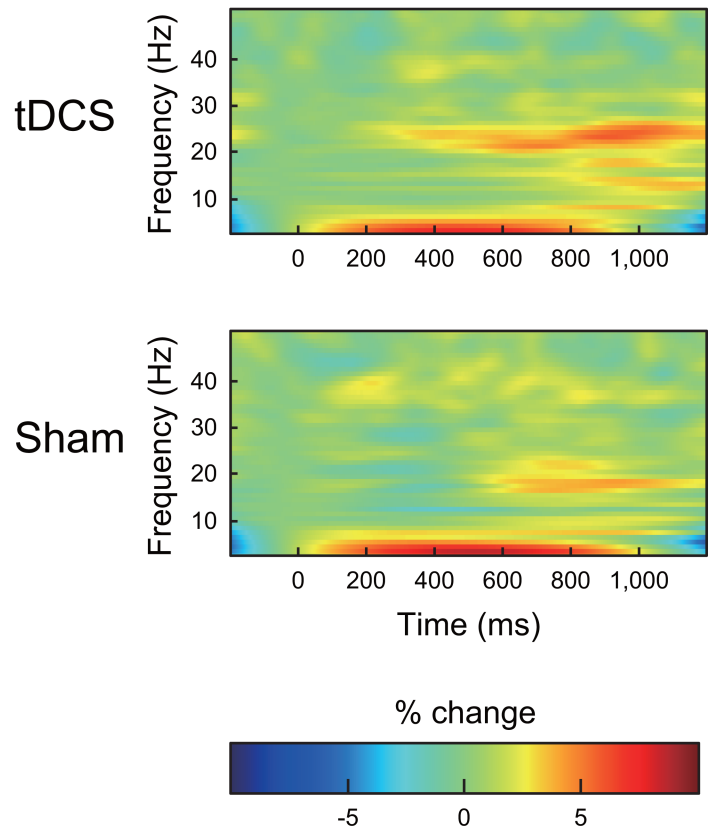
Fig 6. ERSPs in the left precentral gyrus. (A) *T*-maps of the differences in the ERSPs between the tDCS and sham conditions. The threshold of $p < 0.05$ (FDR corrected) is highlighted with a red rectangle. The color indicates the *t*-values at each time-frequency point. Significantly higher ERSPs were observed in the beta-band (20 Hz; a red rectangle) after tDCS than after the sham condition. (B) The grand average of the time-frequency maps of ERSPs in the left precentral gyrus under both tDCS (upper row) and sham (lower row) conditions. In each map, the x-axis indicates time (ms), and the y-axis indicates frequency (Hz). The color indicates ERSPs at each time-frequency point (reflected as the percentage change from baseline).

https://doi.org/10.1371/journal.pone.0193422.g006

Previous studies have focused on the EEG event-related desynchronization (ERD = decreased ERSP) and synchronization (ERS = increased ERSP) in the beta-band during Go/No-Go paradigms [41, 42]. In these studies, No-Go trials displayed an increase in beta power (i.e., ERS) [41, 42]. In addition, one previous study used intracranial recordings and reported that the beta power over the inferior frontal areas increased relative to the baseline during inhibited stop trials but not during failed inhibitions [43]. Therefore, beta-band-enhanced ERSPs likely reflect frontal inhibitory processes. The present study unexpectedly revealed enhanced beta-band ERSPs in the left motor cortex after tDCS compared with that observed after the sham stimuli (Fig 6A; highlighted with a red rectangle). Although the behavioral results in the present study did not reveal an effect of tDCS on the Go/No-Go performance, tDCS with the anode electrode placed over the left frontal area and the cathode electrode placed over the right frontal area might have had an effect on the frontal inhibitory system while the participants were focusing on not pressing the button with their right index finger.

Regarding the tDCS results during the inhibitory task, two previous studies reported the effect of prefrontal tDCS (1.5 mA). Cathodal stimulation of the right dorsolateral prefrontal cortex (DLPFC) increased FAs in healthy subjects during a Go/No-Go task in one study [44]. In another study, cathodal stimulation of the left DLPFC decreased FAs in high school students with attention-deficit/hyperactivity disorder (ADHD) during a Go/No-Go task [45]. Therefore, based on the results from the present study, tDCS applied with the anode electrode placed over the left frontal area and the cathode electrode placed over the right frontal area diminishes the frontal inhibitory processes during Go/No-Go paradigms. However, the results from the present study did not show this effect, i.e., the mean FA per trial was lower under the tDCS conditions (0.20) than under the sham condition (0.38; Wilcoxon signed-rank test, $z = 1.34$, $p > 0.05$, not significant). This inconsistency might be partially explained by the differences in stimulus intensity. Previous studies used lower intensity (1.5 mA) stimuli, whereas we used higher intensity (2 mA) stimuli. One previous study of the motor cortex reported that low-intensity (1 mA) stimulation causes the conventional polarity-specific modulation of neural excitability, whereas high-intensity (2 mA) stimulation leads to increased excitability from both stimulation polarities [46]. In addition to stimulus intensity, the reliability of the induced excitability changes can vary from session to session within individuals and across participants [47]. Because of these uncertain factors in the present study, we might not have observed a significant effect on behavioral performance (i.e., FAs).

Conclusions

In conclusion, the ASSR is an insufficient method to detect the effect of tDCS on cortical NMDA neurotransmission. We unexpectedly observed enhanced beta-band ERSPs in the left motor cortex after tDCS of the frontal area compared with that observed after the sham stimuli. Given that beta-band oscillations reflect many functions in motor cortices, the tDCS for the frontal areas had some effect on the left motor cortex while the participants were focusing on not pressing the button with their right index finger. Further studies with an adequate psychological task (i.e., adequate Go/No-Go proportions) and tDCS of varying intensity and location are necessary to draw conclusions about this unexpected result.

Supporting information

S1 Fig. The grand average of the time-frequency maps for the ERSP in all the ROIs under both tDCS and sham conditions. In each map, the x-axis indicates time (ms), and the y-axis indicates frequency (Hz). The color indicates the ITPCs at each time-frequency point. The ITPC peak in the gamma-band (40 Hz) was clearly observed during the 40 Hz auditory stimulation. (PDF)

S2 Fig. The grand average of the time-frequency maps for the ITPC in all the ROIs under both tDCS and sham conditions. In each map, the x-axis indicates time (ms), and the y-axis indicates frequency (Hz). The color indicates the ITPCs at each time-frequency point. The ITPC peak in the gamma-band (40 Hz) was clearly observed during the 40 Hz auditory stimulation. (PDF)

Author Contributions

Conceptualization: Yoshiaki Miyagishi, Takashi Ikeda, Tetsuya Takahashi, Mitsuru Kikuchi.

Data curation: Takashi Ikeda, Tetsuya Takahashi.

Formal analysis: Yoshiaki Miyagishi, Takashi Ikeda.

References

1. Fox D. Neuroscience: Brain buzz. Nature. 2011; 472(7342):156–8. https://doi.org/10.1038/472156a PMID: 21490649.

2. Kuo MF, Paulus W, Nitsche MA. Therapeutic effects of non-invasive brain stimulation with direct currents (tDCS) in neuropsychiatric diseases. NeuroImage. 2014; 85 Pt 3:948–60. Epub 2013/06/12. https://doi.org/10.1016/j.neuroimage.2013.05.117 PMID: 23747962.

3. Floel A. tDCS-enhanced motor and cognitive function in neurological diseases. NeuroImage. 2014; 85 Pt 3:934–47. https://doi.org/10.1016/j.neuroimage.2013.05.098 PMID: 23727025.

4. Brunoni AR, Moffa AH, Sampaio-Junior B, Borrione L, Moreno ML, Fernandes RA, et al. Trial of Electrical Direct-Current Therapy versus Escitalopram for Depression. N Engl J Med. 2017; 376(26):2523–33. https://doi.org/10.1056/NEJMoa1612999 PMID: 28657871.

5. Brunoni AR, Valiengo L, Baccaro A, Zanao TA, de Oliveira JF, Goulart A, et al. The sertraline vs. electrical current therapy for treating depression clinical study: results from a factorial, randomized, controlled trial. JAMA psychiatry. 2013; 70(4):383–91. https://doi.org/10.1001/2013.jamapsychiatry.32 PMID: 23389323.

6. Coffman BA, Clark VP, Parasuraman R. Battery powered thought: enhancement of attention, learning, and memory in healthy adults using transcranial direct current stimulation. NeuroImage. 2014; 85 Pt 3:895–908. https://doi.org/10.1016/j.neuroimage.2013.07.083 PMID: 23933040.

7. Hill AT, Fitzgerald PB, Hoy KE. Effects of Anodal Transcranial Direct Current Stimulation on Working Memory: A Systematic Review and Meta-Analysis of Findings From Healthy and Neuropsychiatric Populations. Brain stimulation. 2016; 9(2):197–208. https://doi.org/10.1016/j.brs.2015.10.006 PMID: 26597929.

8. Bindman LJ, Lippold OC, Redfearn JW. The Action of Brief Polarizing Currents on the Cerebral Cortex of the Rat (1) during Current Flow and (2) in the Production of Long-Lasting after-Effects. The Journal of physiology. 1964; 172:369–82. PMID: 14199369; PubMed Central PMCID: PMCPMC1368854.

9. Baudewig J, Nitsche MA, Paulus W, Frahm J. Regional modulation of BOLD MRI responses to human sensorimotor activation by transcranial direct current stimulation. Magn Reson Med. 2001; 45 (2):196–201. Epub 2001/02/17. PMID: 11180425.

10. Turi Z, Paulus W, Antal A. Functional neuroimaging and transcranial electrical stimulation. Clin EEG Neurosci. 2012; 43(3):200–8. https://doi.org/10.1177/1550059412444978 PMID: 22956648.

11. Bose A, Shivakumar V, Agarwal SM, Kalmady SV, Shenoy S, Sreeraj VS, et al. Efficacy of fronto-temporal transcranial direct current stimulation for refractory auditory verbal hallucinations in schizophrenia: A randomized, double-blind, sham-controlled study. Schizophrenia research. 2017. https://doi.org/10.1016/j.schres.2017.08.047 PMID: 28866447.

12. Medeiros LF, de Souza IC, Vidor LP, de Souza A, Deitos A, Volz MS, et al. Neurobiological effects of transcranial direct current stimulation: a review. Frontiers in psychiatry. 2012; 3:110. https://doi.org/10.3389/fpsyt.2012.00110 PMID: 23293607; PubMed Central PMCID: PMCPMC3531595.

13. Liebetanz D, Nitsche MA, Tergau F, Paulus W. Pharmacological approach to the mechanisms of transcranial DC-stimulation-induced after-effects of human motor cortex excitability. Brain a journal of neurology. 2002; 125(Pt 10):2238–47. PMID: 12244081.

14. Nitsche MA, Liebetanz D, Schlitterlau A, Henschke U, Fricke K, Frommann K, et al. GABAergic modulation of DC stimulation-induced motor cortex excitability shifts in humans. The European journal of neuroscience. 2004; 19(10):2720–6. https://doi.org/10.1111/j.0953-816X.2004.03398.x PMID: 15147306.

15. Galambos R, Makeig S, Talmachoff PJ. A 40-Hz auditory potential recorded from the human scalp. Proceedings of the National Academy of Sciences of the United States of America. 1981; 78(4):2643–7. PMID: 6941317; PubMed Central PMCID: PMCPMC319406.

16. Kwon JS, O'Donnell BF, Wallenstein GV, Greene RW, Hirayasu Y, Nestor PG, et al. Gamma frequency-range abnormalities to auditory stimulation in schizophrenia. Arch Gen Psychiatry. 1999; 56(11):1001–5. PMID: 10565499; PubMed Central PMCID: PMCPMC2863027.

17. Spencer KM, Salisbury DF, Shenton ME, McCarley RW. Gamma-band auditory steady-state responses are impaired in first episode psychosis. Biological psychiatry. 2008; 64(5):369–75. https://doi.org/10.1016/j.biopsych.2008.02.021 PMID: 18400208; PubMed Central PMCID: PMCPMC2579257.

18. Krishnan GP, Hetrick WP, Brenner CA, Shekhar A, Steffen AN, O'Donnell BF. Steady state and induced auditory gamma deficits in schizophrenia. NeuroImage. 2009; 47(4):1711–9. https://doi.org/10.1016/j.neuroimage.2009.03.085 PMID: 19371786; PubMed Central PMCID: PMCPMC2753273.

19. Hamm JP, Gilmore CS, Clementz BA. Augmented gamma band auditory steady-state responses: support for NMDA hypofunction in schizophrenia. Schizophrenia research. 2012; 138(1):1–7. https://doi.org/10.1016/j.schres.2012.04.003 PMID: 22542616; PubMed Central PMCID: PMCPMC3601795.

20. Rass O, Forsyth JK, Krishnan GP, Hetrick WP, Klaunig MJ, Breier A, et al. Auditory steady state response in the schizophrenia, first-degree relatives, and schizotypal personality disorder. Schizophrenia research. 2012; 136(1–3):143–9. https://doi.org/10.1016/j.schres.2012.01.003 PMID: 22285558; PubMed Central PMCID: PMCPMC3298621.

21. Kirihara K, Rissling AJ, Swerdlow NR, Braff DL, Light GA. Hierarchical organization of gamma and theta oscillatory dynamics in schizophrenia. Biological psychiatry. 2012; 71(10):873–80. https://doi.org/10.1016/j.biopsych.2012.01.016 PMID: 22361076; PubMed Central PMCID: PMCPMC3434875.

22. Hirano Y, Oribe N, Kanba S, Onitsuka T, Nestor PG, Spencer KM. Spontaneous Gamma Activity in Schizophrenia. JAMA psychiatry. 2015; 72(8):813–21. https://doi.org/10.1001/jamapsychiatry.2014.2642 PMID: 25587799; PubMed Central PMCID: PMCPMC4768724.

23. Tada M, Nagai T, Kirihara K, Koike S, Suga M, Araki T, et al. Differential Alterations of Auditory Gamma Oscillatory Responses Between Pre-Onset High-Risk Individuals and First-Episode Schizophrenia. Cerebral cortex. 2016; 26(3):1027–35. https://doi.org/10.1093/cercor/bhu278 PMID: 25452567.

24. Wilson TW, Hernandez OO, Asherin RM, Teale PD, Reite ML, Rojas DC. Cortical gamma generators suggest abnormal auditory circuitry in early-onset psychosis. Cerebral cortex. 2008; 18(2):371–8. https://doi.org/10.1093/cercor/bhm062 PMID: 17557901; PubMed Central PMCID: PMCPMC2648842.

25. Teale P, Collins D, Maharajh K, Rojas DC, Kronberg E, Reite M. Cortical source estimates of gamma band amplitude and phase are different in schizophrenia. NeuroImage. 2008; 42(4):1481–9. https://doi.org/10.1016/j.neuroimage.2008.06.020 PMID: 18634887; PubMed Central PMCID: PMCPMC2637224.

26. Hamm JP, Gilmore CS, Picchetti NA, Sponheim SR, Clementz BA. Abnormalities of neuronal oscillations and temporal integration to low- and high-frequency auditory stimulation in schizophrenia. Biological psychiatry. 2011; 69(10):989–96. https://doi.org/10.1016/j.biopsych.2010.11.021 PMID: 21216392; PubMed Central PMCID: PMCPMC3174270.

27. Tsuchimoto R, Kanba S, Hirano S, Oribe N, Ueno T, Hirano Y, et al. Reduced high and low frequency gamma synchronization in patients with chronic schizophrenia. Schizophrenia research. 2011; 133(1–3):99–105. https://doi.org/10.1016/j.schres.2011.07.020 PMID: 21849245.

28. Edgar JC, Chen YH, Lanza M, Howell B, Chow VY, Heiken K, et al. Cortical thickness as a contributor to abnormal oscillations in schizophrenia? Neuroimage Clin. 2014; 4:122–9. https://doi.org/10.1016/j.nicl.2013.11.004 PMID: 24371794; PubMed Central PMCID: PMCPMC3871288.

29. Thune H, Recasens M, Uhlhaas PJ. The 40-Hz Auditory Steady-State Response in Patients With Schizophrenia: A Meta-analysis. JAMA psychiatry. 2016; 73(11):1145–53. https://doi.org/10.1001/jamapsychiatry.2016.2619 PMID: 27732692.

30. Sivarao DV. The 40-Hz auditory steady-state response: a selective biomarker for cortical NMDA function. Annals of the New York Academy of Sciences. 2015; 1344:27–36. https://doi.org/10.1111/nyas.12739 PMID: 25809615.

31. Sivarao DV, Chen P, Senapati A, Yang Y, Fernandes A, Benitex Y, et al. 40 Hz Auditory Steady-State Response Is a Pharmacodynamic Biomarker for Cortical NMDA Receptors.

Neuropsychopharmacology: official publication of the American College of Neuropsychopharmacology. 2016; 41(9):2232–40. https://doi.org/10.1038/npp.2016.17 PMID: 26837462; PubMed Central PMCID: PMCPMC4946051.

32. Hamalainen M, Hari R, Ilmoniemi RJ, Knuutila J, Lounasmaa OV. Magnetoencephalography—Theory, Instrumentation, and Applications to Noninvasive Studies of the Working Human Brain. Rev Mod Phys. 1993; 65(2):413–97. https://doi.org/10.1103/RevModPhys.65.413 PubMed PMID: WOS: A1993LE48300005.

33. Muthukumaraswamy SD, Singh KD. Visual gamma oscillations: the effects of stimulus type, visual field coverage and stimulus motion on MEG and EEG recordings. NeuroImage. 2013; 69:223–30. https://doi.org/10.1016/j.neuroimage.2012.12.038 PMID: 23274186.

34. Tan HR, Gross J, Uhlhaas PJ. MEG-measured auditory steady-state oscillations show high test-retest reliability: A sensor and source-space analysis. NeuroImage. 2015; 122:417–26. https://doi.org/10.1016/j.neuroimage.2015.07.055 PMID: 26216274.

35. Matsuoka K, Uno M, Kasai K, Koyama K, Kim Y. Estimation of premorbid IQ in individuals with Alzheimer's disease using Japanese ideographic script (Kanji) compound words: Japanese version of National Adult Reading Test. Psychiatry Clin Neurosci. 2006; 60(3):332–9. https://doi.org/10.1111/j.1440-1819.2006.01510.x PMID: 16732750.

36. Monte-Silva K, Kuo MF, Hessenthaler S, Fresnoza S, Liebetanz D, Paulus W, et al. Induction of late LTP-like plasticity in the human motor cortex by repeated non-invasive brain stimulation. Brain stimulation. 2013; 6(3):424–32. https://doi.org/10.1016/j.brs.2012.04.011 PMID: 22695026.

37. Truong DQ, Huber M, Xie X, Datta A, Rahman A, Parra LC, et al. Clinician accessible tools for GUI computational models of transcranial electrical stimulation: BONSAI and SPHERES. Brain stimulation. 2014; 7(4):521–4. https://doi.org/10.1016/j.brs.2014.03.009 PMID: 24776786; PubMed Central PMCID: PMCPMC4108562.

38. Tadel F, Baillet S, Mosher JC, Pantazis D, Leahy RM. Brainstorm: a user-friendly application for MEG/EEG analysis. Comput Intell Neurosci. 2011; 2011:879716. Epub 2011/05/18. https://doi.org/10.1155/2011/879716 PMID: 21584256; PubMed Central PMCID: PMC3090754.

39. Huang MX, Mosher JC, Leahy RM. A sensor-weighted overlapping-sphere head model and exhaustive head model comparison for MEG. Phys Med Biol. 1999; 44(2):423–40. Epub 1999/03/10. PMID: 10070792.

40. Pascual-Marqui RD. Standardized low-resolution brain electromagnetic tomography (sLORETA): technical details. Methods and findings in experimental and clinical pharmacology. 2002; 24 Suppl D:5–12. PMID: 12575463.

41. Alegre M, Gurtubay IG, Labarga A, Iriarte J, Valencia M, Artieda J. Frontal and central oscillatory changes related to different aspects of the motor process: a study in go/no-go paradigms. Experimental brain research. 2004; 159(1):14–22. https://doi.org/10.1007/s00221-004-1928-8 PMID: 15480586.

42. Leocani L, Toro C, Zhuang P, Gerloff C, Hallett M. Event-related desynchronization in reaction time paradigms: a comparison with event-related potentials and corticospinal excitability. Clinical neurophysiology: official journal of the International Federation of Clinical Neurophysiology. 2001; 112(5):923–30. PMID: 11336910.

43. Swann N, Tandon N, Canolty R, Ellmore TM, McEvoy LK, Dreyer S, et al. Intracranial EEG reveals a time- and frequency-specific role for the right inferior frontal gyrus and primary motor cortex in stopping initiated responses. The Journal of neuroscience: the official journal of the Society for Neuroscience. 2009; 29(40):12675–85. https://doi.org/10.1523/JNEUROSCI.3359-09.2009 PMID: 19812342; PubMed Central PMCID: PMCPMC2801605.

44. Beeli G, Casutt G, Baumgartner T, Jancke L. Modulating presence and impulsiveness by external stimulation of the brain. Behav Brain Funct. 2008; 4:33. https://doi.org/10.1186/1744-9081-4-33 PMID: 18680573; PubMed Central PMCID: PMCPMC2529286.

45. Soltaninejad Z, Nejati V, Ekhtiari H. Effect of Anodal and Cathodal Transcranial Direct Current Stimulation on DLPFC on Modulation of Inhibitory Control in ADHD. J Atten Disord. 2015. https://doi.org/10.1177/1087054715618792 PMID: 26689935.

46. Batsikadze G, Moliadze V, Paulus W, Kuo MF, Nitsche MA. Partially non-linear stimulation intensity-dependent effects of direct current stimulation on motor cortex excitability in humans. The Journal of physiology. 2013; 591(7):1987–2000. https://doi.org/10.1113/jphysiol.2012.249730 PMID: 23339180; PubMed Central PMCID: PMCPMC3624864.

47. Horvath JC, Carter O, Forte JD. Transcranial direct current stimulation: five important issues we aren't discussing (but probably should be). Frontiers in systems neuroscience. 2014; 8:2. https://doi.org/10.3389/fnsys.2014.00002 PMID: 24478640; PubMed Central PMCID: PMCPMC3901383.